Journal of Structural Chemistry, Vol. 40, No. 4, 1999

SIZE AND STRUCTURE OF MOLECULAR CLUSTERS IN SUPERCRITICAL WATER

S. V. Churakov and A. G. Kalinichev

UDC 539.266/532.74

The type and topology of hydrogen-bonded molecular clusters of water are investigated by the molecular dynamics method for five models of water in supercritical conditions. Small clusters (of the order of 10 molecules) are present in all models, even at densities of less than 0.2 g/cm^3. When the density increases, a phase transition occurs from vapor-like to fluid-like state. Among small clusters, linear structures are predominant.

INTRODUCTION

In the near-critical region, the thermodynamic properties of water undergo substantial changes within a narrow range of temperatures and pressures. These near-critical anomalies must be closely related to pronounced qualitative changes in the structure of the fluid [1]. Structural relationships in a water fluid are mainly determined by the presence of hydrogen bonds between water molecules. In supercritical conditions, the continuous net of hydrogen bonds existing in liquid water in normal conditions is considerably destructed. However, as shown by recent analyses of the results of both experimental works and computer simulations [2-4], hydrogen bonds still affect the structure and properties of supercritical water, linking the individual molecules into more or less large multimolecular clusters.

In this connection, detailed quantitative analysis of the size and structure of such clusters seems important. Recent investigations showed that isotope exchange and ionic liquid–vapor fractionation depend heavily on the extent of clusterization of water molecules [5]. Moreover, the greatest effect on the liquid–vapor equilibrium is expected from structural changes in a low-dense phase [6].

Here the results of a molecular dynamic (MD) computer simulation of the properties of supercritical water [7] are used to analyze the distribution of hydrogen-bonded molecular clusters varying in size according to the temperature and density of supercritical fluid and to study the topological and structural characteristics of the most widespread clusters such as trimers, tetramers, and pentamers.

MD CALCULATION PROCEDURE

For the molecular dynamic simulation we used the standard algorithm of microcanonical (NVE) ensemble [8]. The systems under investigation consisted of $N = 200$ water molecules in a cubic unit cell whose dimensions were varied from one calculation to another to set the required density. Standard periodic boundary conditions were employed. The range of densities $0.17 < \rho < 1.28$ g/cm^3 corresponds to pressures from 25 to 3300 MPa. Altogether we studied 5 thermodynamic states at temperatures from 623 to 773 K.

The intermolecular interaction was modeled with a nonrigid potential BJH [9], which allowed us to study the effects of variation in temperature, density, and local molecular environment on many properties of water at a fundamental atomic molecular level [7, 10]. Due to the inner degrees of freedom inherent in the BJH potential as well as some special requirements for the stability of the computation algorithm in modeling high-temperature supercritical states, the equations of motion for molecules were integrated with a very small time step of $\Delta\tau = 1.5\times10^{-16}$ s. The long-range

M. V. Lomonosov Moscow State University. Institute of Experimental Mineralogy, Russian Academy of Sciences (Chernogolovka). Translated from *Zhurnal Strukturnoi Khimii*, Vol. 40, No. 4, pp. 673-680, July-August, 1999. Original article submitted June 11, 1998.

 0022-4766/99/4004-0548$22.00

TABLE 1. Thermodynamic Parameters of MD Calculations for Water

MD calculation	*A*	*B*	*C*	*D*	*E*
Temperature, K	673	772	630	680	771
Density, g/cm^3	0.167	0.528	0.693	0.972	1.284
Pressure, MPa	25	100	57	630	3260

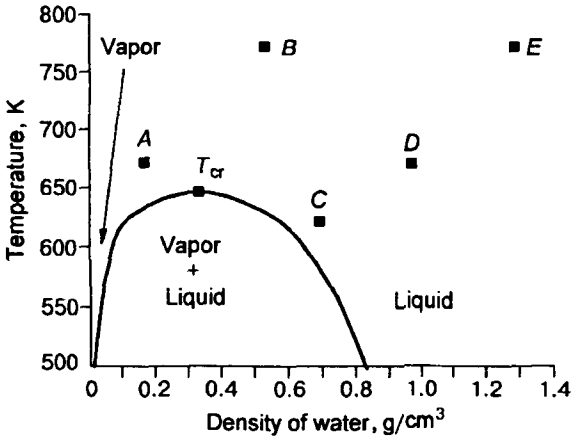

Fig. 1. Fragment of the phase diagram of water in the near-critical region. The dots show the conditions of MD calculations (Table 1).

Coulomb interaction was included in the calculation using Ewald's version of summation; for all other interactions, the shifted force method was employed [8]. The equilibrium properties of each thermodynamic state were calculated by time averaging for a trajectory of more than 15,000 steps in length after preliminary equilibration of about the same period of time. Detailed analyses of the thermodynamic, structural, kinetic, and spectroscopic results of these MD experiments and of the translational and librational dynamics of individual water molecules and self-diffusion coefficients in supercritical conditions were published in [7, 10]. The same communications give a detailed account of the computation algorithm.

To investigate the distributions of molecular clusters in supercritical water according to size and structure we used a few hundred equilibrium molecular configurations in each case for the thermodynamic parameters listed in Table 1 in the order of increasing density. In Fig. 1, the points under study are plotted on the phase diagram of water. For the given thermodynamic states, Table 1 also lists the pressures calculated by Saul–Wagner's equation of state [11]. The parameters of the points *A*, *B*, *D*, *E* lie above the critical point of water, and the point *C* is in the vicinity of the liquid–vapor equilibrium curve (Fig. 1). It should be taken into account that the liquid–vapor equilibrium curves may differ dramatically between the real and "computed" water with the BJH potential. Thus, in one of acceptable situations, the point *C* lies in the two-phase region of the phase diagram in the BJH model.

In the configuration analysis, the *i*th and *j*th molecules were considered hydrogen-bonded if they satisfied the combined space-energy criterion of H-bond [3, 12], which is reduced to two conditions: 1) the distance between the O atom of the *i*th molecule and the H atom of the *j*th molecule is $R_{O...H} \le R_{HB}$; 2) the pair energy of interaction between the atoms is $E_{ij} \le E_{HB}$. Here $R_{HB} = 2.4$ Å is the maximal length of the hydrogen bond, and $E_{HB} = -10$ kJ/mole is its minimal (in the absolute value) energy. The molecule was considered belonging to the cluster if it had at least one such bond with the other molecules of the cluster. It should be emphasized that instant configurations of water molecules (so-called *I*-structures) were analyzed.

RESULTS AND DISCUSSION

Before passing to the analysis of the results, recall several methodological characteristics of computer simulation. Small size of model systems is one of the main features distinguishing them from natural substances. In our case, the

cell contained 200 molecules, which naturally limited the size of the structures to be analyzed. Detection of clusters of 180 or more molecules may be indicative of the presence of an infinite continuous net of hydrogen bonds in the macroscopic system. Nevertheless, it is yet premature to anambiguously answer the question concerning the minimal cluster size admitting the existence of an infinite molecular net. For systems under analysis, the minimal size is 100-150 molecules. One can take the relation $N_C = N/2$ as a rough estimate of this limit; here N_C is the number of molecules in the cluster, and N is the total number of molecules in the system under study.

The presence (or absence) of an infinite molecular cluster in the system may be estimated more exactly by comparing the average number of hydrogen bonds per molecule in the given thermodynamic state with the percolation threshold, which is $n = 1.6$ for an arbitrary net of tetrahedrally ordered bonds [13]. In our calculations, the points A and B obviously refer to the region below the percolation threshold, and the points D and E refer to the region above the percolation threshold [3].

Size and distribution of water clusters. The estimations generally used to determine the average number of hydrogen bonds per water molecule [2-4, 12] do not answer the question about the size and form of hydrogen-bonded clusters. Using the results of an MD computer simulation, we calculated the average number of molecules involved in the formation of clusters of different sizes (Fig. 2).

The temperature difference between the points B, E and A, D is of the order of 100°. However, in the case of supercritical parameters, the temperature differences may often be neglected [7, 10]; below we discuss only the influence of the increased density of the fluid on the redistribution of water molecules between different types of cluster.

As would be expected, the greater the density of a fluid, the larger the clusters formed. It should be noted that there is a radical difference in the character of the cluster distribution of molecules between the points A, B and E, B corresponding to the relatively low and high densities, respectively. In the region of low densities (points A, B), only small clusters are found. However, even in relatively low-dense vapor (point A), one can find clusters of up to 10 molecules; at moderate densities (point B), clusters of 20 and more molecules are frequent.

Calculations at higher densities give two clear-cut maxima corresponding to the presence of both small (up to 15 molecules) and very large (more than 150 molecules) clusters. Remarkably, no molecular structures of intermediate size are found between the two peaks. Therefore, it is safe to assume that the peak of a cluster of 150-200 molecules is due to an infinite dynamic cluster. The left peak on the diagram corresponds to molecular groups which, at the moment of the analysis, were torn away from the single continuous net of hydrogen bonds, and it is not improbable that at next moments of time these clusters will merge with larger ones.

The character of distribution at point C is different. Here we observe structures of any size. The absence of clusters of definite size merely suggests inadequate statistics for the configurations studied; improved statistics will evidently lead to a continuous and bimodal distribution. One of the peaks is very distinct and corresponds to solitary molecules and small clusters; another peak is very diffuse and has a maximum in the interval between 110 and 150 molecules; it is probably formed from the products of decomposition of larger clusters. The specific properties of this distribution suggest that the physicochemical parameters at point C may correspond to the two-phase state of water in the BJH model. This distribution seems to reflect the liquid–vapor transition, during which the infinite net of hydrogen bonds inherent in the fluid-like state decomposes into single molecules and low-molecular clisters characteristic of a low-dense phase.

In supercritical conditions, the macroscopic liquid–vapor phase transition does not take place. However, as can be seen from the diagrams in Fig. 2, when the density increases, the inner structure of the fluid is radically transformed, suggesting a certain similarity of phase transition at a microlevel. The picture discovered completely supports the previous conclusions drawn from the analysis of the thermodynamic properties (in particular, pressure) calculated for the BJH model and from the position of the maximum of the intramolecular stretching vibrations for point C [7, 10].

Topological characteristics of the clusters. In this paper, we restricted ourselves to a topology analysis of relatively small clusters containing 3, 4, and 5 molecules. The topological types of cluster revealed in the analysis are schematically shown in Fig. 3.

The histograms in Fig. 4 show the relative distributions of molecular configurations for the given 3-, 4-, and 5-molecular clusters, respectively. For the five points under study, the relative distributions are very similar.

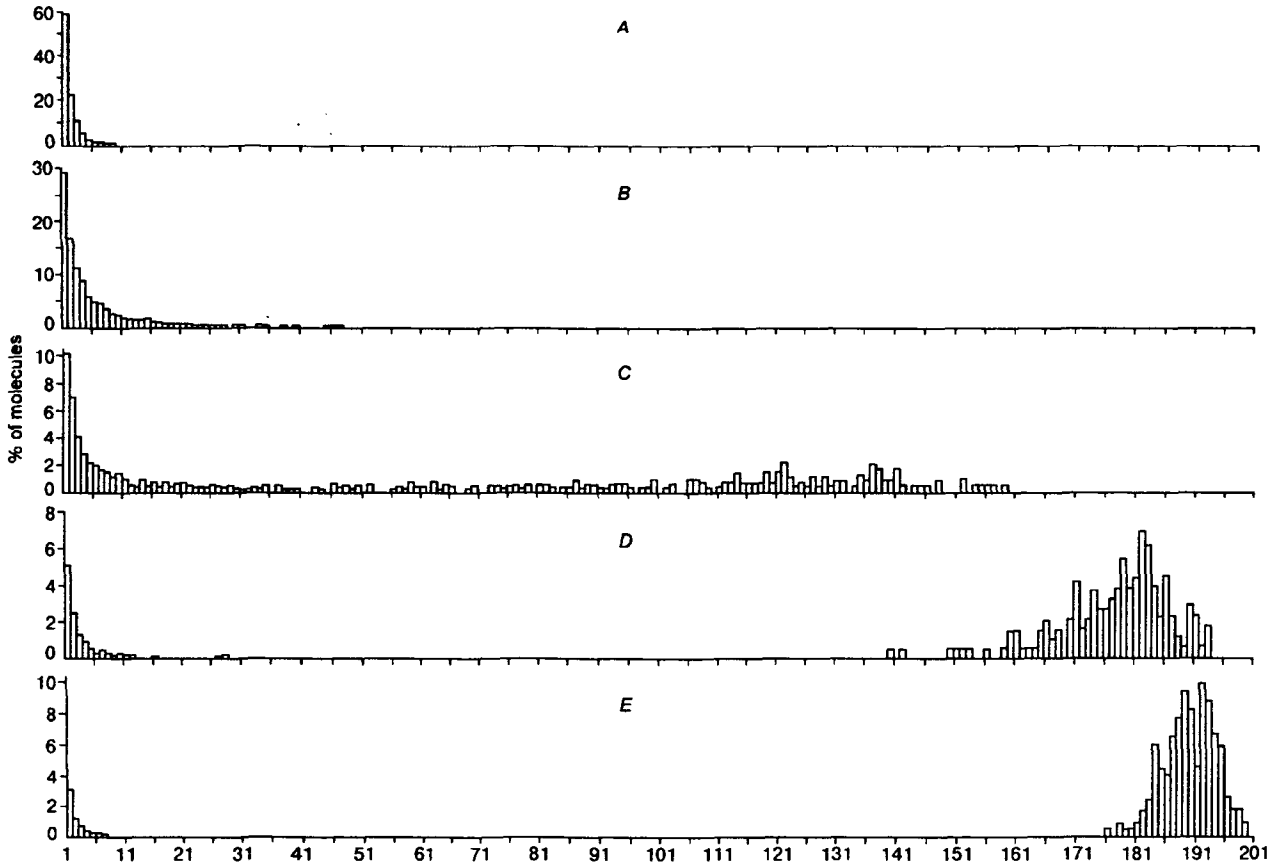

Fig. 2. Histograms of the distribution of water molecules according to clusters of different size (in percent of the total number of molecules) for different conditions (Table 1). Density: *A* – 0.167, *B* – 0.528, *C* – 0.693, *D* – 0.972, *E* – 1.284 g/cm^3.

Complex structures were found along with simple (for example, linear) clusters, which are predominant. It should be borne in mind that we considered instant molecular configurations. Some of the structures may be the products of accidental high-velocity collisions of several molecules or of simple clusters with separate molecules possessing a high kinetic energy. These configurations may be comparatively short-lived and not possessing the lifetime characteristic of the hydrogen bond. It should be emphasized, however, that all these configurations satisfy both the energy and the geometry criteria of the hydrogen bond and are not energetically unfavorable.

Three-molecular clusters (Fig. 3, *A*; Fig. 4, *A*). Only two types of trimer: chain and three-membered ring are topologically possible. More than 99% of the total number of trimers are chains. This is not surprising, since formation of a three-membered ring requires too extensive deformation of all the three hydrogen bonds of the cluster, which is evidently energetically unfavorable.

Four-molecular clusters (Fig. 3 *B*; Fig. 4, *B*). In systems of 4 molecules, 6 topological types of intermolecular bond can exist. Using the results of simulation, we found only 4 types of cluster. In the histogram presented in Fig. 4, it can be seen that unbranched chains predominate among the tetramer structures (80.1%). Clusters No. *3* (Fig. 4) are less numerous (16.9%). Configurations of type 4 (Fig. 3, *B*) constitute about 2.5%; type 2 (Fig. 3, *B*) is represented by less than 0.5%.

Five-molecular clusters (Fig. 3, *C*; Fig. 4, *C*). A system of five molecules can form 14 topological types of cluster. The majority of these types are energetically unfavorable and may not be realized. In the analysis of molecular configurations we came across only six types of structure whose distribution histogram is presented in Fig. 4, *C*. As in the previous case, unbranched molecular chains are predominant (62.8% of all the observed pentamers). Then follow clusters No. *2* (Fig. 3, *C*) (34.9%). The other 4 structural types amount to less than 2.3% and are distributed extremely irregularly at calculation points. This group of structures must also be assigned to very short-lived objects.

It is interesting to note that the data on the real topology of molecular clusters in supercritical water differ

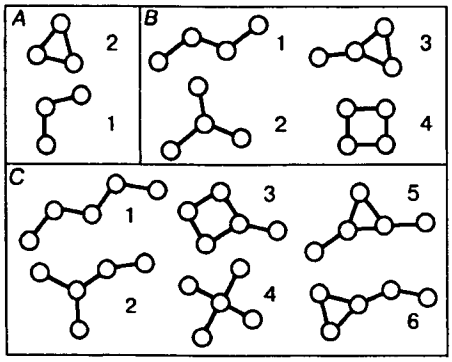

Fig. 3. Schematic drawing showing the topological types of cluster. The circles correspond to water molecules; the black lines symbolize hydrogen bonds between molecules.

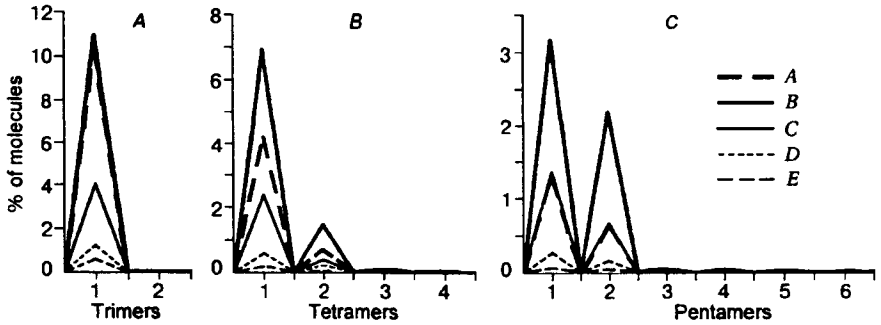

Fig. 4. Histograms of the distribution of different topological types among the three- (*A*), four- (*B*), and five-molecular (*C*) clusters for different thermodynamic conditions (Table 1). The numbers of structural types correspond to the clusters shown in Fig. 3.

significantly from the results of quantum mechanical calculations. It was shown [14, 15] that, among pentamers, a molecular structure in the form of a closed ring possesses minimal potential energy. In our study, five-membered rings were not reported at all. A simple explanation to this discrepancy is the difference between the calculation conditions; at supercritical temperatures, the high kinetic energy of molecules hinders formation of stable ring structures. This is supported by MD calculations [14], in which closed five-membered rings proved to be unstable even at near-room temperatures.

The above analysis showed that no pentamers organized into complete tetrahedral clusters (Fig. 3, *C*, No. *4*) exist even at high densities. At first sight, this contradicts the experimental X-ray diffraction data in supercritical water [16], indicating a peak of pairwise molecular distribution of the tetrahedrally ordered water molecules even in the thermodynamic conditions corresponding to point *B* in our calculations. However, this is a seeming contradiction, because the fragments of a tetrahedrally ordered net of hydrogen bonds responsible for the indicated peak are easily found in all of the observed clusters starting from trimers, and the absence of clusters in the form of complete isolated tetrahedra, as in the case of ring structures, may be explained by their extreme instability at supercritical temperatures.

CONCLUSIONS

Thus our study shows that

1. Even at relatively low densities (less than 0.2 g/cm^3), supercritical water contains a great number of comparatively large clusters (up to 10 molecules per cluster).

2. In the supercritical region, when the density increases and the state of water changes from the low-density

vapor-like state (single small clusters) to the high-density liquid-like fluid (infinite cluster above the percolation threshold), a transition analogous to the phase transition of condensation takes place in a narrow range of densities.

3. No relationship has been found between the density and the distributions of various topological types of low-molecular clusters.

4. A distribution analysis for various structural types revealed the predominance of linear clusters. No ring molecular structures have been found among the pentamolecular clusters, while the fraction of the pentamers in the form of complete tetrahedra is very insignificant.

We are grateful to Dr. Yu. E. Gorbatyi for his interest in our work and useful discussions. This work was supported by RFFR grant No. 97-03-32587a, CRDF grant No. RC1-170, and INTAS grant Nos. UA-95-0096 and 96-1989.

REFERENCES

1. Yu. E. Gorbatyi, A. G. Kalinichev, and G. V. Bondarenko, *Nature*, No. 8, 78-89 (1997).
2. Yu. E. Gorbatyi and A. G. Kalinichev, *J. Phys. Chem.*, **99**, 5336-5340 (1995).
3. A. G. Kalinichev and J. D. Bass, *ibid.*, **101**, 9720-9727 (1997).
4. A. G. Kalinichev and Yu. E. Gorbatyi, *Experimental and Theoretical Simulation of Mineral Formation Processes* [in Russian], Nauka, Moscow (1998), pp. 242-264.
5. T. Dreisner, *Science*, **277**, 791-794 (1997).
6. Y. Gussiani and B. Guillot, *J. Chem. Phys.*, **98**, 8221-8235 (1993).
7. A. G. Kalinichev and K. Heinzinger, *Geochim. Cosmochim. Acta*, **59**, 641-650 (1995).
8. M. P. Allen and D. J. Tildesley, *Computer Simulation of Liquids*, Oxford University, New York (1987).
9. P. Bopp, G. Jancso, and K. Heinzinger, *Chem. Phys. Lett.*, **98**, 129-133 (1983).
10. A. G. Kalinichev, *Ber. Bunseng. Phys. Chem.*, **97**, 872-876 (1993).
11. A. Saul and W. Wagner, *J. Phys. Chem. Ref. Data*, **18**, 1537-1564 (1989).
12. A. G. Kalinichev and J. D. Bass, *Chem. Phys. Lett.*, **231**, 301-307 (1994).
13. R. L. Blumberg, H. E. Stanley, A. Geiger, and P. Mausbach, *J. Chem. Phys.*, **80**, 5230-5241 (1984).
14. P. L. M. Plummer and T. S. Chen, *ibid.*, **86**, 7149-7156 (1987).
15. K. S. Kim, M. Dupuis, G. C. Lie, and E. Clementi, *Chem. Phys. Lett.*, **131**, 451-454 (1986).
16. Yu. E. Gorbatyi and Yu. N. Dem'yanets, *ibid.*, **100**, 450-455 (1983).